Enriching red emission of $Y_3Al_5O_{12}$: Ce^{3+} by codoping Pr^{3+} and Cr^{3+} for improving color rendering of white LEDs

Lei Wang,[1,2] Xia Zhang,[1] Zhendong Hao,[1] Yongshi Luo,[1] Xiao-jun Wang,[3] and Jiahua Zhang[1,*]

[1]*Key Laboratory of Excited State Processes, CIOMP, Chinese Academy of Sciences, 3888 Eastern South Lake Road, Changchun 130033, China*
[2]*Graduate School of Chinese Academy of Sciences, Beijing 100039, China*
[3]*Department of Physics, Georgia Southern University, Statesboro, Georgia 30460, USA*
**zhangjh@ciomp.ac.cn*

Abstract: Triply doped $Y_3Al_5O_{12}$: Ce^{3+}, Pr^{3+}, Cr^{3+} phosphors are prepared by solid state reaction. The emission spectra are enriched in the red region with the luminescence of both Pr^{3+} and Cr^{3+} through $Ce^{3+}\rightarrow Cr^{3+}$ and $Ce^{3+}\rightarrow Pr^{3+}\rightarrow Cr^{3+}$ energy transfers. The properties of photoluminescence and fluorescence decay indicates larger macroscopic $Ce^{3+}\rightarrow Cr^{3+}$ transfer rates in the triply doped phosphors in comparison to Ce^{3+} and Cr^{3+} doubly doped one, reflecting the effect of competition between $Ce^{3+}\rightarrow Cr^{3+}$ and $Ce^{3+}\rightarrow Pr^{3+}$ transfers. White LEDs fabricated using the triply doped phosphor coated on blue LED chips show a color rendering index of 81.4 higher than that either using Ce^{3+} and Cr^{3+} doubly doped or Ce^{3+} singly doped phosphor.

OCIS codes: (160.5690) Rare-earth-doped materials; (260.2160) Energy transfer; (250.5230) photoluminescence; (230.3670) Light-emitting diodes.

References and links

1. J. K. Kim, and E. F. Schubert, "Transcending the replacement paradigm of solid-state lighting," Opt. Express **16**(26), 21835–21842 (2008).
2. J. R. Oh, S. H. Cho, Y. H. Lee, and Y. R. Do, "Enhanced forward efficiency of $Y_3Al_5O_{12}$:Ce^{3+} phosphor from white light-emitting diodes using blue-pass yellow-reflection filter," Opt. Express **17**(9), 7450–7457 (2009).
3. R. Mueller-Mach, G. O. Mueller, M. R. Krames, and T. Trottier, "High-Power Phosphor-Converted Light-Emitting Diodes Based on III-Nitrides," IEEE J. Sel. Top. Quantum Electron. **8**(2), 339–345 (2002).
4. H. S. Jang, W. B. Im, D. C. Lee, D. Y. Jeon, and S. S. Kim, "Enhancement of red spectral emission intensity of Y 3 Al 5 O 12:Ce^{3+} phosphor via Pr co-doping and Tb substitution for the application to white LEDs," J. Lumin. **126**(2), 371–377 (2007).
5. H. H. Yang, and Y. S. Kim, "Energy transfer-based spectral properties of Tb-, Pr-, or Sm-codoped YAG:Ce nanocrystalline phosphors," J. Lumin. **128**(10), 1570–1576 (2008).
6. Y. Pan, M. Wu, and Q. Su, "Tailored photoluminescence of YAG:Ce phosphor through various methods," Phys. Chem. Solids **65**(5), 845–850 (2004).
7. W. Wang, J. Tang, S. T. V. Hsu, J. Wang, and B. P. Sullivan, "Energy transfer and enriched emission spectrum in Cr and Ce co-doped $Y_3Al_5O_{12}$ yellow phosphors," Chem. Phys. Lett. **457**(1-3), 103–105 (2008).
8. K. M. Kinsman, J. McKittrick, E. Sluzky, and K. Hesse, "Phase Development and Luminescence in Chromium-Doped Yttrium Aluminum Garnet (YAG:Cr) Phosphors," J. Am. Ceram. Soc. **77**(11), 2866–2872 (1994).
9. G. G. Özen, O. Forte, and B. Di Bartolo, "Down-conversion and upconversion dynamics in Pr-doped $Y_3Al_5O_{12}$ crystals," J. Appl. Phys. **97**(1), 013510 (2005).
10. G. G. Özen, O. Forte, and B. Di Bartolo, "Upconversion dynamics in Pr-doped $YAlO_3$ and $Y_3Al_5O_{12}$ laser crystals," Opt. Mater. **27**(11), 1664–1671 (2005).
11. M. Malinowski, P. Szczepanski, W. Woliński, R. Wolski, and Z. Frukacz, "Inhomogeneity study of Pr^{3+}-doped yttrium aluminium garnet using time-resolved spectroscopy," J. Phys. Condens. Matter **5**(35), 6469–6482 (1993).
12. Y. R. Shen, and K. L. Bray, "Effect of pressure and temperature on the lifetime of Cr^{3+} in yttrium aluminum garnet," Phys. Rev. B **56**(17), 10882–10891 (1997).
13. W. W. Jia, H. Liu, S. Jaffe, W. M. Yen, and B. Denker, "Spectroscopy of Cr^{3+} and Cr^{+4} ions in forsterite," Phys. Rev. B **43**(7), 5234–5242 (1991).

#134729 - $15.00 USD Received 8 Sep 2010; revised 24 Oct 2010; accepted 28 Oct 2010; published 17 Nov 2010

1. Introduction

Phosphor-converted white light–emitting diodes (pcWLEDs) are potential replacements for conventional light sources such as incandescent or fluorescent lamps [1]. The general strategy for producing pcWLED is to combine blue LED with the yellow emitting $Y_3Al_5O_{12}$: Ce^{3+} (YAG: Ce^{3+}) phosphor at present [2]. However, YAG: Ce^{3+} has relatively weak emission in the red spectral region, leading to color rendering index (CRI) of pcWLEDs below 80. To meet the requirement of higher CRIs (> 80) for general illumination, co-doping red emitting ions as co-activators into YAG: Ce^{3+} was extensively studied [3–7]. Mueller-Mach and associates [3] added Pr^{3+} into YAG:Ce^{3+} to replace Y and consequently obtained a red emission line at 608 nm, originating from $^1D_2 \rightarrow {}^3H_4$ transition of Pr^{3+}, through energy transfer from Ce^{3+} to Pr^{3+}. However, increasing Pr^{3+} concentration over 0.015 for obtaining enough red components leads to a notable decrease of the red line due to self concentration quenching [4,5]. Recently, Wang et al. [7] selected Cr^{3+} as an red emitting center to incorporate into YAG: Ce^{3+} phosphor to replace Al sites [8] and observed a deep red emission line of Cr^{3+} at about 690 nm through $Ce^{3+} \rightarrow Cr^{3+}$ energy transfer. While, no notable luminescence quenching of Cr^{3+} was observed for high Cr^{3+} concentration. Unsatisfactorily, both doubly doped YAG: Ce^{3+}, Pr^{3+} and YAG: Ce^{3+}, Cr^{3+} phosphors still need more red spectral component for high color rendering white LEDs because YAG: Ce^{3+}, Pr^{3+} lacks for emission in deep red spectral region and YAG: Ce^{3+}, Cr^{3+} lacks in light red region.

In this paper, we prepared triply doped YAG: Ce^{3+}, Pr^{3+}, Cr^{3+} phosphors by solid state reaction. The performance of energy transfer among these emitting centers leads to simultaneous observation of yellow emission from Ce^{3+}, light red emission from Pr^{3+} and deep red emission from Cr^{3+} upon blue light excitation. The white LEDs fabricated using the triply doped phosphor shows higher CRI than that using singly or doubly doped YAG phosphors.

2. Experimental

Powder phosphor samples were made using mixtures of high-purity Y_2O_3, CeO_2, Al_2O_3, Cr_2O_3 and Pr_6O_{11} in molar of $(Y_{1-z-y}Ce_zPr_y)_3$ $(Al_{1-x}Cr_x)_5O_{12}$ (x, y, z represent the concentration of Cr^{3+}, Pr^{3+} and Ce^{3+}, respectively), and fired under CO reducing condition at 1500°C for 3 h. The structure of the final products is characterized by powder X-ray diffraction (XRD). Photoluminescence (PL) and photoluminescence excitation (PLE) spectra are measured with a Hitachi Spextra-fluorometer (F-4500). The decay of the fluorescence from Ce^{3+} is measured by an FL920 fluorometer with a hydrogen flash lamp. In the measurements of fluorescence decay of Pr^{3+} and Cr^{3+}, an optical parametric oscillator (OPO) is used as an excitation source. The signal is detected by a Tektronix digital oscilloscope (TDS 3052).

3. Results and discussion

Figure 1 shows the PL and PLE spectra of Ce^{3+}, Pr^{3+}, Cr^{3+} singly (a,b), doubly (d,e) and triply (f) doped YAG. The Ce^{3+} singly doped sample exhibits a well known yellow emission band peaking at around 530 nm due to the transition from the lowest-lying 5d state to the 4f ground state of Ce^{3+}. The PLE spectrum of the yellow band consists of a band at 470 nm corresponding to the transition from the ground state to the lowest-lying 5d state, and two ultraviolet (UV) PLE bands corresponding to the upper 5d states, located at 340 nm and 230 nm, respectively [2], as shown in Fig. 1(a). The Pr^{3+} singly doped sample exhibits three groups of emissions of Pr^{3+} upon 288 nm excitation, as shown in Fig. 1(b). The group in the UV region consists of two strong bands located at 317 nm and 381 nm, which are originated to the transitions from the lowest lying 4f5d state to ^3H_J (J = 4, 5, 6) and the ^3F_J (J = 2, 3, 4) manifolds, respectively [9]. The group in the range of 450 – 600 nm originates from $^3P_0 \rightarrow {}^3H_{4,5}$ transitions dominated by a intense blue emission line at 488 nm due to $^3P_0 \rightarrow {}^3H_4$ transition. The other group in red originates from $^1D_2 \rightarrow {}^3H_4$ transitions dominated by a intense emission line at 608 nm with a weak satellite line at 640nm [10,11]. The PLE spectra of the three groups of emissions in Pr^{3+}

#134729 - $15.00 USD Received 8 Sep 2010; revised 24 Oct 2010; accepted 28 Oct 2010; published 17 Nov 2010

singly doped sample are identical in the UV spectral range, showing two 4f5d PLE bands located at 288 nm and 238 nm, respectively. In Fig. 1(c), the principal features of the PLE spectra of Cr^{3+} singly doped sample are a $O^{2-} - Cr^{3+}$ related charge transfer band (CTB) peaking at 230nm and three broad bands peaking at 280nm, 443nm and 608nm, which belong to the spin-allowed electronic transitions from the $^4A_2$ to the $^4T_1$ (4 P), $^4T_1$ (4 F) and $^4T_2$ (4 F) states, respectively. The PL spectra are the typical emissions of Cr^{3+}, which contains a $^2E - {}^4A_2$ zero-phonon line peaking at 685 nm with vibronic sidebands [12,13]. In Fig. 1(d), the PL spectrum of Ce^{3+} and Cr^{3+} doubly doped sample contains not only the yellow band of Ce^{3+} but also the red bands of Cr^{3+} when only Ce^{3+} is excited at 340 nm. Furthermore, the PLE spectrum monitoring Cr^{3+} 685nm emission includes two typical Ce^{3+} absorption bands at 340nm and 470nm, demonstrating occurrence of $Ce^{3+} \rightarrow Cr^{3+}$ energy transfer. In the Fig. 1(e), the PL spectrum of Pr^{3+} and Cr^{3+} doubly doped sample exhibits Cr^{3+} typical emissions at 685nm as Pr^{3+} is only excited by 288 nm and the PLE spectrum monitoring the Cr^{3+} emission shows a clear Pr^{3+} absorption band at 288nm, indicating $Pr^{3+} \rightarrow Cr^{3+}$ energy transfer. The PL spectrum of triply doped sample exhibits all typical emissions of Ce^{3+}, Pr^{3+} and Cr^{3+} when only Ce^{3+} is excited at 340 nm, as shown in Fig. 1(f). This is the result of $Ce^{3+} \rightarrow Cr^{3+}$, $Ce^{3+} \rightarrow Pr^{3+}$ and $Pr^{3+} \rightarrow Cr^{3+}$ energy transfers. The emission spectrum is considerably enriched in the red region with the luminescence of both Pr^{3+} and Cr^{3+}.

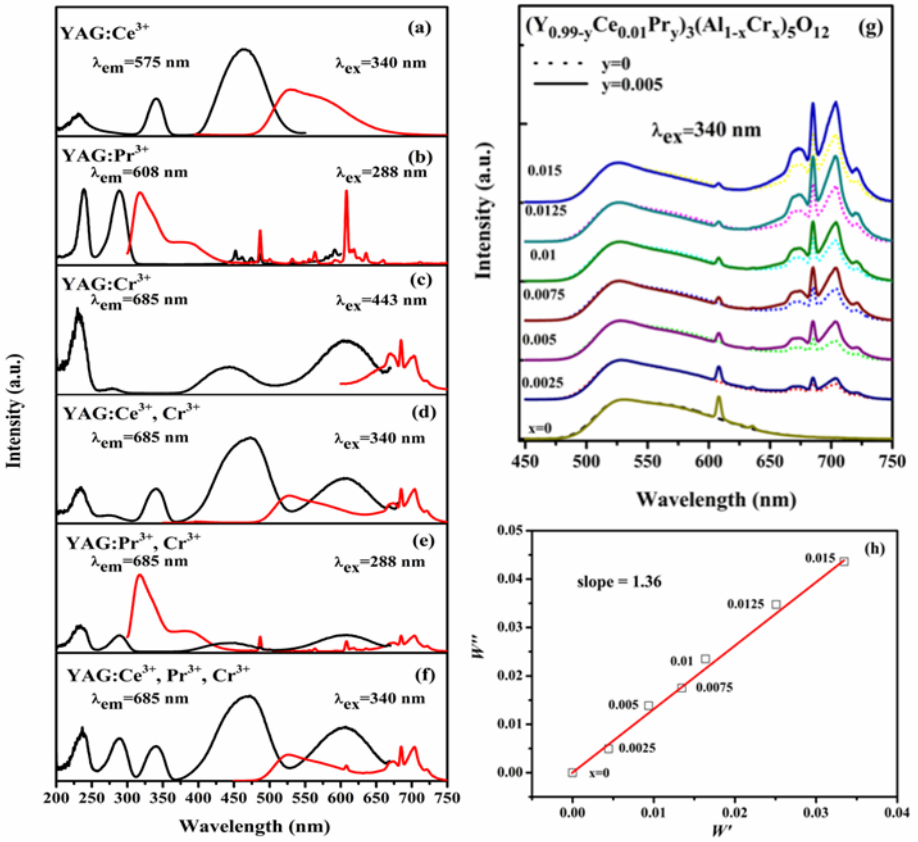

Fig. 1. PL and PLE spectra of $(Y_{0.99}Ce_{0.01})_3Al_5O_{12}$ (a), $(Y_{0.99}Pr_{0.005})_3Al_5O_{12}$ (b), $Y_3(Al_{0.9925}Cr_{0.0075})_5O_{12}$ (c), $(Y_{0.99}Ce_{0.01})_3(Al_{0.9925}Cr_{0.0075})_5O_{12}$ (d), $(Y_{0.99}Pr_{0.005})_3(Al_{0.9925}Cr_{0.0075})_5O_{12}$ (e) and $(Y_{0.985}Ce_{0.01}Pr_{0.005})_3(Al_{0.9925}Cr_{0.0075})_5O_{12}$ (f); PL spectra of $(Y_{0.99-y}Ce_{0.01}Pr_y)_3(Al_{1-x}Cr_x)_5O_{12}$, (x = 0, 0.0025, 0.005, 0.0075, 0.01, 0.0125, 0.015; y = 0 (dashed curves), 0.005 (solid curves)). The intensity of the yellow band in each spectrum is normalized(g); Dependence of *W''* of triply doped samples series A on *W'* of doubly doped samples series B(h).

#134729 - $15.00 USD Received 8 Sep 2010; revised 24 Oct 2010; accepted 28 Oct 2010; published 17 Nov 2010

Figure 1(g) shows PL spectra of triply doped sample series A (solid): $(Y_{0.985}Ce_{0.01}Pr_{0.005})_3(Al_{1-x}Cr_x)_5O_{12}$ and Ce^{3+}, Cr^{3+} doubly doped sample series B (dotted): $(Y_{0.99}Ce_{0.01})_3(Al_{1-x}Cr_x)_5O_{12}$ with variable Cr^{3+} concentration x in the range of 0 ~0.015 upon Ce^{3+} excitation at 340 nm. All spectra are normalized to the yellow band. The deep red emission of Cr^{3+} grows up with increasing x, reflecting the increase of the $Ce^{3+}\rightarrow Cr^{3+}$ energy transfer efficiency since Cr^{3+} cannot be excited directly by 340 nm. When the upper 5d state of Ce^{3+} is excited at 340 nm, a rapid relaxation down to the lowest 5d state performs and subsequently the energy is transferred from Ce^{3+} to Cr^{3+}.

Table 1. Fluorescent lifetimes and transfer efficiencies in $(Y_{0.99}Ce_{0.01})_3(Al_{1-x}Cr_x)_5O_{12}$ and $(Y_{0.985}Ce_{0.01}Pr_{0.005})_3(Al_{1-x}Cr_x)_5O_{12}$

x	$(Y_{0.99}Ce_{0.01})_3(Al_{1-x}Cr_x)_5O_{12}$			$(Y_{0.985}Ce_{0.01}Pr_{0.005})_3(Al_{1-x}Cr_x)_5O_{12}$		
	5d of Ce^{3+} τ_{Ce} (ns)	^4E of Cr^{3+} τ_{Cr} (μs)	$W' = 1/\tau_{Ce}-1/\tau_{Ce,0}$ (1/ns)	5d of Ce^{3+} τ_{Ce} (ns)	^4E of Cr^{3+} τ_{Cr} (μs)	$W'' = 1/\tau_{Ce}-1/\tau_{Ce,0}$ (1/ns)
	λ_{ex} = 340 nm	λ_{ex} = 355nm		λ_{ex} = 340nm	λ_{ex} = 355nm	
	λ_{em} = 530nm	λ_{em} = 700nm		λ_{em} = 530nm	λ_{em} = 700nm	
0	57.8		0	46		0
0.0025	46	1794	0.00444	37.5	1845	0.00493
0.005	37.5	1715	0.00937	28.1	1750	0.01385
0.0075	32.5	1717	0.01347	25.5	1660	0.01748
0.01	29.7	1555	0.01637	22.1	1544	0.02351
0.0125	23.6	1508	0.02507	17.7	1411	0.03476
0.015	19.7	1404	0.03346	15.3	1296	0.04362

One can find in Fig. 1(g) that the deep red emission of Cr^{3+} in the triply doped phosphor is always stronger than that in doubly doped one for the same x. To understand this behavior, we have measured the decay curves of the yellow fluorescence of Ce^{3+} and the deep red fluorescence of Cr^{3+} in both sample series A and B. The lifetimes of the yellow fluorescence (τ_{Ce}) and the red fluorescence (τ_{Cr}) are calculated by integrating the area under the corresponding decay curves with a normalized initial intensity, as listed in Table 1. The lifetimes τ_{Ce} become shorter with increasing x, implying the enhanced $Ce^{3+}\rightarrow Cr^{3+}$ energy transfer. The macroscopic $Ce^{3+}\rightarrow Cr^{3+}$ energy transfer rate, W can be evaluated by

$$W = 1/\tau_{Ce} - 1/\tau_{Ce,0}. \quad (1)$$

In continuous excitation, the steady state rate equation concerning the population, n_{Ce}, of the lowest 5d state of Ce^{3+} and, n_{Cr}, of the ^2E state of Cr^{3+} is written as $Wn_{Ce} = n_{Cr}/\tau_{Cr}$. The intensity ratio ($I_{Cr}/I_{Ce}$) of Cr^{3+} to Ce^{3+} emission is proportional to $W\tau_{Cr}$, as expressed by

$$I_{Cr} / I_{Ce} = (\gamma_{Cr} / \gamma_{Ce}) W \tau_{Cr}, \quad (2)$$

where the radiative transiton rate γ's are considered to be independent on Cr^{3+} concentration.

We found in Table 1 that the macroscopic $Ce^{3+}\rightarrow Cr^{3+}$ energy transfer rate, *W''*, in the triply doped samples is always larger than *W'* in Ce^{3+} and Cr^{3+}doubly doped one for the same x. This phenomenon can be well explained as described below. In the triply doped samples, the presence of Pr^{3+} shortens the intrinsic lifetime of the Ce^{3+} fluorescence from 57.8 ns to 46 ns due to $Ce^{3+}\rightarrow Pr^{3+}$ energy transfer. As Cr^{3+} is added, there is a competition between $Ce^{3+}\rightarrow Pr^{3+}$ energy transfer and $Ce^{3+}\rightarrow Cr^{3+}$ energy transfer. The Ce^{3+} ions with small $Ce^{3+}\rightarrow Cr^{3+}$ energy transfer rates are easily transferred to Pr^{3+}, so that the Ce^{3+} ions in the excited state upon continuous excitation contain a larger number of fast Ce^{3+} ions in the presence of Pr^{3+} in comparison to the case of Pr^{3+} free. Therefore, a larger macroscopic $Ce^{3+}\rightarrow Cr^{3+}$ energy transfer rate is expected in the triply doped samples. As we plot *W''* versus its corresponding *W'*, they well satisfy a proportional relationship with a slope 1.36, as shown in Fig. 1(h). It means the value of *W''* is about 1.36 times that of *W'* for the same x. From Eq. (2), the intensity ratio (I_{Cr}/I_{Ce}) is proportional to $W\tau_{Cr}$. Taking into account the τ_{Cr} that exhibits a small difference

#134729 - $15.00 USD Received 8 Sep 2010; revised 24 Oct 2010; accepted 28 Oct 2010; published 17 Nov 2010

between doubly and triply doped samples for the same x, it is evaluated that the intensity of Cr^{3+} emission in the triply doped samples [solid in Fig. 1(g)] should be averagely 1.32 times that in doubly doped samples [dotted in Fig. 1(g)] for the same x. We find in Fig. 1(g) that the ratio is around 1.59 larger than 1.32. While noticing the reduction of the red line at 608 nm of Pr^{3+} with increasing x, we attribute the extra ratio to the contribution made by $Pr^{3+}\rightarrow Cr^{3+}$ energy transfer. In this case, the components of the deep red emission of Cr^{3+} in the triply doped samples are provided by not only $Ce^{3+}\rightarrow Cr^{3+}$, but also $Pr^{3+}\rightarrow Cr^{3+}$ energy transfer.

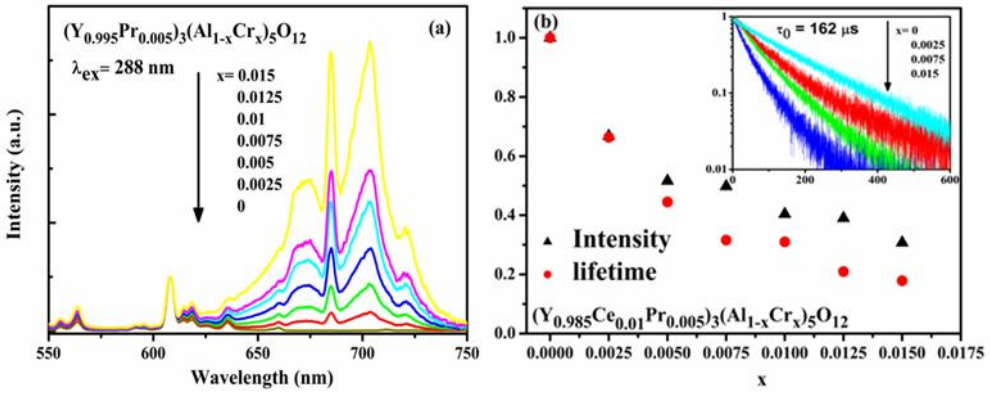

Fig. 2. (a) PL spectra of $(Y_{0.995}Pr_{0.005})_3(Al_{1-x}Cr_x)_5O_{12}$, (x = 0, 0.0025, 0.005, 0.0075, 0.01, 0.0125, 0.015) under 288 nm excitation. The intensity of the pale red peak in each spectrum is normalized; (b) Pr^{3+} red fluorescence intensity and lifetime changed with increasing Cr^{3+} concentration x in $(Y_{0.985}Pr_{0.005}Ce_{0.01})_3(Al_{1-x}Cr_x)_5O_{12}$. Inset shows decay curves of the pale red fluorescence in $(Y_{0.985}Pr_{0.005}Ce_{0.01})_3(Al_{1-x}Cr_x)_5O_{12}$ for x = 0, 0.0025, 0.0075 and 0.015.

To study the effect of $Pr^{3+}\rightarrow Cr^{3+}$ energy transfer, Pr^{3+}, Cr^{3+} doubly doped sample series C: $(Y_{0.995}Pr_{0.005})_3(Al_{1-x}Cr_x)_5O_{12}$ with variable Cr^{3+} concentration x (x = 0 ~0.015) are synthesized. Figure 2(a) shows the PL spectra of sample series C as only Pr^{3+} is excited at 288 nm. All spectra are normalized by the intensity of Pr^{3+} $^1D_2\rightarrow{}^3H_4$ red line. The PL spectra present enhancement of Cr^{3+} emission with increasing x due to $Pr^{3+}\rightarrow Cr^{3+}$ energy transfer, which also results in shortening of the lifetimes of Pr^{3+} $^1D_2$ as presented in the insert of Fig. 2(b). The decay curves (insert) of the $^1D_2$ is measured by monitoring at 608 nm upon pulsed excitation at 288 nm. A descending dependence of Pr^{3+} emission intensities and its lifetimes on x are plotted in Fig. 2(b). They fit well for small x, but that the Pr^{3+} red emission intensity reduces faster than its lifetime for x higher than 0.005. This is considered to be the result of reabsorption of the red line by the spin-allowed $^4A_2 - {}^4T_2$ (4 F) transition of Cr^{3+}.

According to the PL spectra in Fig. 2(a), the deep red component provided by $Pr^{3+}\rightarrow Cr^{3+}$ energy transfer in the triply doped samples [see Fig. 1(g)] can be estimated from the corresponding intensity of the red line of Pr^{3+}. Figure 3(a) shows x dependence of I_{Cr}/I_{Ce} with its two components (One is fed by $Ce^{3+}\rightarrow Cr^{3+}$ energy transfer. Another one is fed by $Pr^{3+}\rightarrow Cr^{3+}$ energy transfer) in the triply doped samples. The component fed by $Ce^{3+}\rightarrow Cr^{3+}$ energy transfer is evaluated from I_{Cr}/I_{Ce} in Ce^{3+} and Cr^{3+} doubly doped samples multiplied by 1.32. Figure 3(a) demonstrates that the combination of the two components is in a good agreement with the total intensity of the deep red emission of Cr^{3+}.

To test the triply doped phosphors, $(Y_{0.98}Ce_{0.02})_3Al_5O_{12}$, $(Y_{0.98}Ce_{0.02})_3(Al_{0.999}Cr_{0.001})_5O_{12}$ and $(Y_{0.978}Ce_{0.02}Pr_{0.002})_3(Al_{0.999}Cr_{0.001})_5O_{12}$ phosphors are selected to fabricate LEDs using the blue InGaN LED chips. The electroluminescence (EL) emission spectra of the white LEDs measured under a forward-bias current of 20 mA is shown in Fig. 3(b). The color coordinates and the color rendering indices (CRI) of the fabricated white LED are listed in Table 2. The CRI of the white LED fabricated with the triply doped phosphor is 81.4 that is higher than 80.4 fabricated using the doubly doped phosphor and 78.3 using the singly doped phosphor. The luminous efficiency

#134729 - $15.00 USD Received 8 Sep 2010; revised 24 Oct 2010; accepted 28 Oct 2010; published 17 Nov 2010

of the present white LEDs fabricated with singly, doubly and triply doped phosphors are 99.2 lm/W, 88.3 lm/W and 84.3 lm/W, respectively, yielding the luminous efficiency for the triply doped phosphor around 85% of the singly doped one. For the luminescence quantum yield of the triply doped phosphor that is not measured in this work could be higher than 85% of YAG:Ce^{3+} in view of vision function are insensitive to red light.

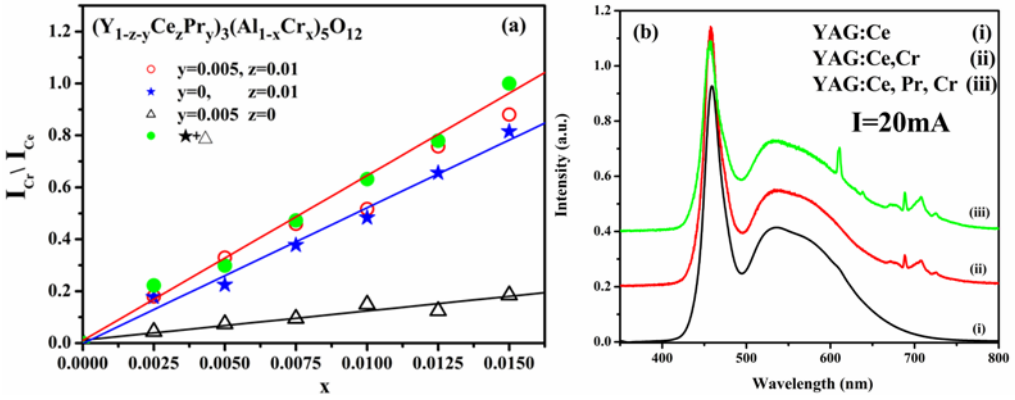

Fig. 3. (a) Dependence of the emission ratio (I_{Ce}/I_{Cr}) on Cr^{3+} concentration x in $(Y_{1-z-y}Ce_zPr_y)_3(Al_{1-x}Cr_x)_5O_{12}$; (b) EL spectra of the white LEDs using different phosphors coated on InGaN-based blue chips.

Table 2. Optical properties of white LED

	color coordinates		CRI
	x	y	
$(Y_{0.98}Ce_{0.02})_3Al_5O_{12}$	0.2893	0.3266	78.3
$(Y_{0.98}Ce_{0.02})_3(Al_{0.999}Cr_{0.001})_5O_{12}$	0.2844	0.3111	80.4
$(Y_{0.978}Ce_{0.02}Pr_{0.002})_3(Al_{0.999}Cr_{0.001})_5O_{12}$	0.2974	0.3323	81.4

4. Conclusions

$Y_3Al_5O_{12}$: Ce^{3+}, Pr^{3+}, Cr^{3+} phosphors are prepared by solid state reaction. Three typical emission bands: yellow emission from Ce^{3+}, light red emission from Pr^{3+} and deep red emission from Cr^{3+} are achieved upon blue light excitation on Ce^{3+}. The study of photoluminescence and fluorescence decay indicates that there are $Ce^{3+}\rightarrow Cr^{3+}$ and $Ce^{3+}\rightarrow Pr^{3+}\rightarrow Cr^{3+}$ energy transfers. For the same Cr^{3+} concentration, the macroscopic $Ce^{3+}\rightarrow Cr^{3+}$ energy transfer rate in the triply doped phosphor is larger than that in the doubly doped one, which is attributed to the competition between $Ce^{3+}\rightarrow Pr^{3+}$ energy transfer and $Ce^{3+}\rightarrow Cr^{3+}$ energy transfer. A white LED fabricated using a blue LED chip with the triply doped phosphor shows a color rendering index of 81.4 that is higher than that either using Ce^{3+}, Cr^{3+} doubly doped or Ce^{3+} singly doped phosphors.

Acknowledgements

This work is financially supported by the National Nature Science Foundation of China (10834006, 10774141, 10904141, 10904140), the MOST of China (2006CB601104), the Scientific project of Jilin province (20090134, 20090524) and CAS Innovation Program.

#134729 - $15.00 USD Received 8 Sep 2010; revised 24 Oct 2010; accepted 28 Oct 2010; published 17 Nov 2010